



PAPER

OPEN ACCESS

RECEIVED
21 January 2020REVISED
18 February 2020ACCEPTED FOR PUBLICATION
25 February 2020PUBLISHED
16 March 2020

Original content from this work may be used under the terms of the [Creative Commons Attribution 4.0 licence](#).

Any further distribution of this work must maintain attribution to the author(s) and the title of the work, journal citation and DOI.



Transition in nanoscale electrical conductivity in the Langmuir-Blodgett film of a novel liquid crystalline oligomer

Bharat Kumar^{1,3} , K A Suresh², Hari Krishna Bisoyi³ and Sandeep Kumar^{3,4}¹ Department of Physics, Central University of Karnataka, Kadaganchi, Kalaburagi—585 367, India² Centre for Nano and Soft Matter Sciences, Prof. U. R. Rao Road, P.B. No: 1329, Jalahalli, Bengaluru—560 013, India³ Raman Research Institute, Sadashivanagar, Bengaluru-560080, India⁴ Department of Chemistry, NITTE Meenakshi Institute of Technology (NMIT), P.B. No. 6429, Yelahanka, Bengaluru-560064, IndiaE-mail: bharat@cuk.ac.in**Keywords:** metal-semiconductor-metal junction, self assembly at interfaces, current sensing atomic force microscopy, liquid crystals

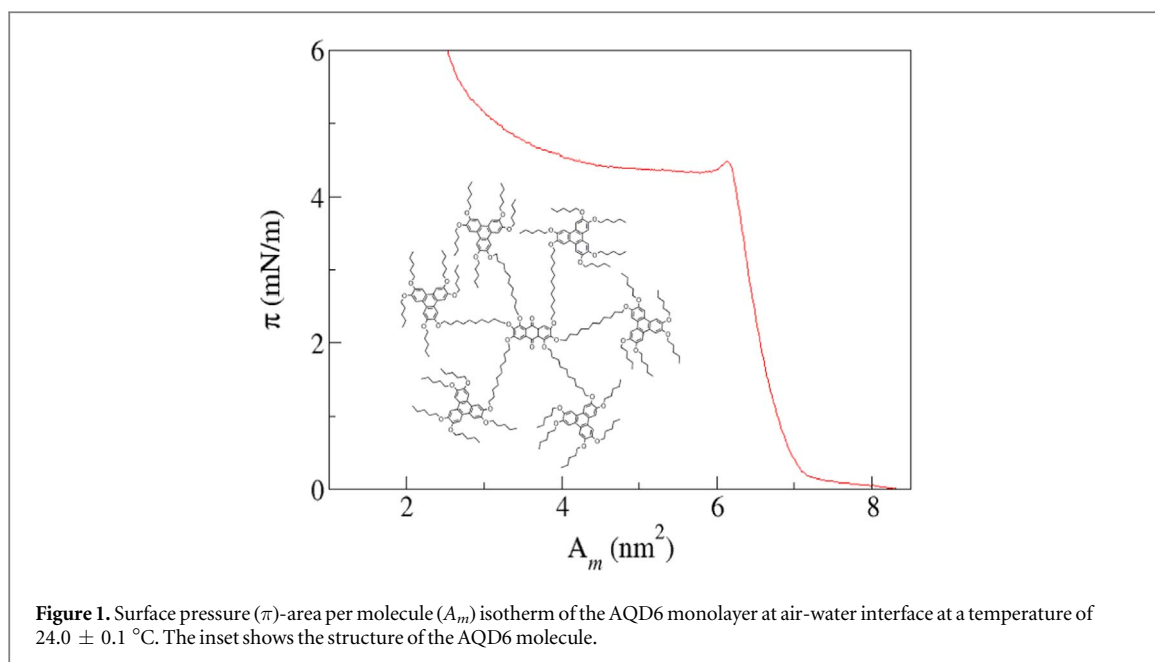
Abstract

We have studied the nanoscale electrical conductivity of a monolayer film of a novel star shaped liquid crystalline molecule, hexatriphenylene substituted anthraquinone (AQD6). The molecule has a central core of electron deficient anthraquinone moiety connected to six electron rich triphenylene moieties by flexible alkyl chains. The monolayer formed at air-water interface was transferred onto the solid substrates by Langmuir-Blodgett (LB) technique and its surface topography was imaged using an atomic force microscope (AFM). The limiting area obtained from the surface pressure-area per molecule isotherm and the topography of the AFM images suggest that the anthraquinone moiety of the AQD6 molecule is organized in face-on configuration on the substrate and the triphenylene moieties are in edge-on configuration extended away from the substrate. We have studied the electrical conductivity of the AQD6 monolayer deposited on gold coated silicon substrate using a current sensing AFM. Analysis of current (I) – voltage (V) characteristics of the metal-monolayer film-metal junction showed a transition from direct tunneling to an injection tunneling. Further, we have estimated the barrier height and the effective mass of electron in the metal-monolayer film-metal junction.

1. Introduction

Organic materials with electron rich and electron deficient groups are interesting because of their unique electrical [1, 2] and optical [3, 4] properties. Thin films of these materials find technological applications in the field effect transistors, light-emitting diodes and photo-voltaic devices [5, 6]. For such applications, the molecules must be well ordered in the thin film [7], since the structure and morphology of the film are important in fabricating the devices. Amphiphilic organic molecules can self-assemble at air-water interface to yield well ordered monolayer known as Langmuir monolayer. These ordered monolayers can be transferred onto solid substrates by Langmuir-Blodgett (LB) technique and it is one of the convenient methods to prepare thin film of organic molecules with good ordering and orientation. Molecular ordering can also be obtained by the process of self organization [8]. Combination of the phenomenon of self organization along with the LB technique can give well oriented and highly ordered thin films [9]. In this context, novel amphiphilic molecules containing discotic moieties are interesting, since the $\Pi - \Pi$ stacking of the disk shaped cores in the LB film can result in the formation of two dimensional anisotropic structures [10, 11]. The LB film of liquid crystalline molecules with different cores like anthraquinone [6], triphenylene [12–15] and phthalocyanine [16] have been studied.

Understanding the electrical properties of thin films of well ordered molecules is important for wide range of applications in organic electronics. Studies have been carried out in this direction and many interesting results have emerged. Song *et al* [17] have studied the monolayers of octadecanedithiol and benzenedithiol and showed



that there is a transition in the charge transfer mechanism through the monolayer depending on the bias voltage applied across the film. Such systems can be used as molecular transistors [17] where, the charge transport through the molecules can be controlled by appropriately modulating the molecular orbitals using an external electrical field. Similar studies on other organic molecules sandwiched between two electrodes suggests that coupling between electrodes and organic thin film affects the charge transfer mechanism through metal-film-metal junction [18–21]. In this regard, it is important to study the metal-film-metal junction with the well ordered molecules in the film having different molecular orbital structure is important. The presence of electron rich and deficient moieties in the molecules improves in charge transfer through the molecules in the film after tunnelling from the electrode [3, 12]. In addition, the asymmetry in the structure of the molecules will result in asymmetric metal-film junctions and hence the resulting metal-film-metal junctions may have characteristics of a rectifier, which is interesting for many molecular device applications. In the presence of low applied bias voltage between the electrodes, the electrons directly tunnel between the electrodes. However, for high voltages, when the Fermi level of the electrode is close to the HOMO or LUMO levels of the film, the charges are first injected into the film from an electrode and they are further transferred through the film before escaping into the other electrode.

We have studied the Langmuir monolayer and LB films of a novel star shaped liquid crystalline molecule, hexatriphenylene substituted anthraquinone (AQD6) (inset of figure 1). The molecule has a central core of electron deficient anthraquinone which is connected to six disk shaped, electron rich triphenylene moieties by flexible alkyl chains. These molecules with electron rich and electron deficient moieties, can have interesting electrical properties when organized in a thin film. The limiting area obtained from the surface pressure-area per molecule isotherm of the AQD6 monolayer at air-water interface and the atomic force microscope (AFM) images of the LB film suggest that the anthraquinone moiety is in face-on configuration on the substrate and the six triphenylene moieties are extended away from the substrate in edge-on configuration. We have studied the nanoscale electrical conductivity of the monolayer film on a gold coated silicon substrate using a current sensing atomic force microscope (CSAFM). The monolayer film between AFM cantilever tip and substrate forms a metal-film-metal junction, where the film introduces a potential barrier for the electron transfer. Our analysis of the current (I) – voltage (V) characteristics indicated that the current flow across the junction is through the process of electron tunneling. Further, as the bias voltage is increased gradually, we find a transition in the tunneling mechanism, from direct tunneling to injection tunneling.

2. Experimental

The material AQD6 was synthesized in our laboratory [22]. It was purified by repeated column chromatography and the purity was found to be better than 99% as indicated by NMR, IR and elemental analyzer techniques. The structure of the molecule is shown in figure 1. The Langmuir monolayer film at air-water interface was studied by surface manometry and Brewster angle microscopy (BAM). The surface manometry studies were carried out using a Nima trough (Model: 611M). Ultra-pure deionized water of resistivity greater than 18 M Ω cm (millipore

water, MilliQ) and pH 5.7 was used as subphase. The monolayer was compressed at a rate of about $22 \text{ \AA}^2 \text{ molecule}^{-1} \text{ min}^{-1}$. The experiments were carried out at a temperature of $24.0 \text{ }^\circ\text{C}$. The BAM studies were carried out using MiniBAM (NFT, Nanotech).

The monolayer film of AQD6 molecules was prepared by transferring the monolayer from air-water interface by LB technique onto different solid substrates like mica, hydrophilic silicon and gold coated silicon. The mica sheet was freshly cleaved before the transfer of the film. To obtain hydrophilic silicon substrates, the polished silicon wafers were treated with boiling piranha solution (3: 1 ratio of concentrated sulphuric acid and hydrogen peroxide) for about 5 min. The transfer of the monolayer was carried out at a surface pressure of 4 mN/m , with a dipping speed of 2 mm/min . Mica sheet, hydrophilic silicon and gold coated silicon being hydrophilic substrates, they get coated with one layer of the film in one dipping cycle (consisting of one downstroke and one upstroke) [23]. The transfer of the film occurred during upstroke. Surface morphology and thickness of the LB film were obtained from the AFM studies (Model:PicoPlus, Molecular Imaging). The film was scanned in the AC mode using silicon cantilevers with nominal values of resonance frequency 175 kHz and spring constant 30 N/m .

The nanoscale electrical conductivity of the AQD6 monolayer on a gold coated silicon substrate was studied using CSAFM. Platinum coated silicon cantilevers (Appnano) with a spring constant in the range of $0.02\text{--}0.8 \text{ N/m}$ were used. The tip radius was about 30 nm . The polished silicon substrate was coated with pure gold by thermal evaporation. The evaporation was carried out at a pressure of 10^{-4} torr and the thickness of the gold film was between $80\text{--}100 \text{ nm}$. The conducting tip and the gold coated silicon substrate act like two metal electrodes separated by the AQD6 monolayer film. The bias voltage was applied to the substrate and the tip was kept at virtual ground. A preamplifier with an operational range of 1 pA to 10 nA was connected to the tip to measure the signal. The noise level in our system was about 10 pA and a current higher than this value was measurable. The film was scanned in the contact mode with a constant applied force and the topography and current images were acquired simultaneously. The force applied by the tip on the film and the bias voltage values were suitably chosen to avoid any damage to the film during the scan.

3. Results and discussion

The material AQD6 was studied under a polarizing microscope. The material exhibits liquid crystalline phase at room temperature and melted to isotropic phase on heating to $123 \text{ }^\circ\text{C}$. On cooling from isotropic phase, the sample transformed to a liquid crystalline phase at $116 \text{ }^\circ\text{C}$ and continued to be in that phase upto about $15 \text{ }^\circ\text{C}$. The x-ray characterization of the liquid crystalline phase indicated that the molecules are stacked one above the other to form a hexagonal columnar phase [22].

3.1. Surface manometry and Brewster angle microscopy

Surface pressure (π)–area per molecule (A_m) isotherm of the AQD6 monolayer at air-water interface is shown in figure 1.

At large A_m the isotherm shows zero surface pressure. On compression, around 7.0 nm^2 the π value sharply increases. At an A_m of 6.2 nm^2 , the monolayer collapsed with a collapse pressure of about 4.3 mN/m . The stability of the monolayer was checked by holding the barriers at a constant A_m and monitoring the π as a function of time. We find the monolayer to be stable for A_m values above 6.2 nm^2 .

The BAM studies showed the phases exhibited by the AQD6 monolayer at different A_m values (figure 2).

Figure 2(a) represents the BAM image at large A_m showing the coexistence of dark and grey regions. Between A_m values of 7.0 nm^2 and 6.2 nm^2 , the monolayer exhibited a uniform phase (figure 2(b)). On further compression, the monolayer collapsed exhibiting bright 3-dimensional striations coexisting with dark and grey regions (figure 2(c)).

The uniform phase exhibited by the monolayer can be characterized by calculating the compressional modulus ($|E|$) using the relation [24],

$$|E| = A_m \frac{d\pi}{dA_m} \quad (1)$$

Here, $d\pi/dA_m$ is the variation of π as a function of A_m . Figure 3 shows the variation of $|E|$ as a function of A_m .

The compressional modulus has a maximum value of 32 mN/m , which corresponds to a low density liquid (L_1) phase of the monolayer [24, 25]. Hence, from the $\pi - A_m$ isotherm, $|E|$ value and BAM images, we infer that above an A_m of 7.0 nm^2 , the monolayer exhibited coexisting gas and L_1 phase and between 7.0 nm^2 and 6.2 nm^2 , it exhibited a uniform L_1 phase before collapsing. The limiting area per molecule A_o , which gives the area occupied by the molecule in the monolayer has a value of 6.8 nm^2 , as obtained from the $\pi - A_m$ isotherm.

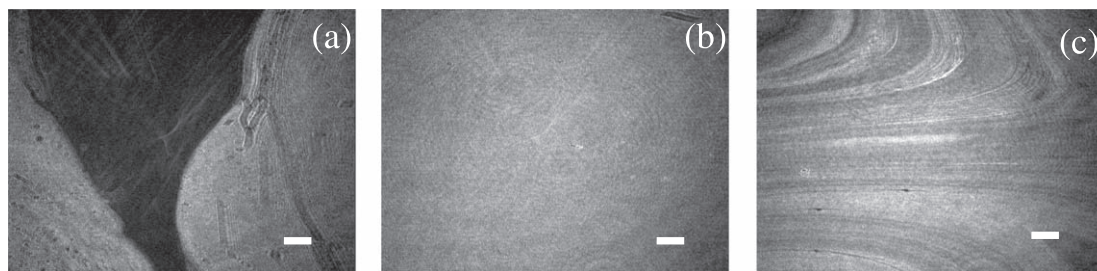


Figure 2. BAM images of the AQD6 monolayer at different area per molecule. (a) Shows coexistence of gas and liquid expanded phase at $A_m = 7.60 \text{ nm}^2$. (b) Shows uniform liquid expanded phase at $A_m = 6.65 \text{ nm}^2$. (c) Shows the collapsed state at $A_m = 4.40 \text{ nm}^2$. The scale bar in each image represents $500 \mu\text{m}$.

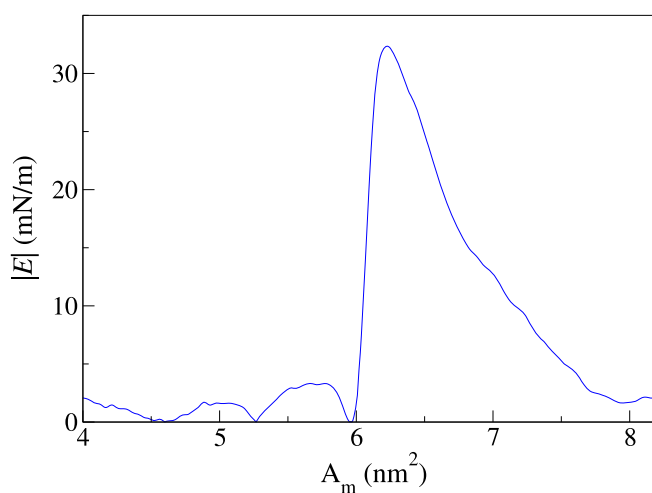


Figure 3. Plot of compressional modulus ($|E|$) as a function of area per molecule (A_m). The maximum value of $|E|$ is about 32 mN/m at A_m of 6.2 nm^2 . This value of $|E|$ corresponds to the liquid expanded phase of the monolayer.

3.2. Atomic force microscopy

The LB film of AQD6 monolayer on solid substrates of mica and hydrophilic silicon was studied using AFM in the non contact mode. The transfer ratio of the film transferred onto a hydrophilic mica substrate was about 0.85. Figure 4 shows the AFM topography image of the LB monolayer on the mica substrate.

The line profile on the topography image yields a height of about 3.4 nm . The length of the triphenylene moiety substituted with the alkyl chains (pentyl chain) is estimated (using ChemDraw) to be about 2.0 nm . The length of the alkyl chains (dodecyl chain) connecting the triphenylene moieties with the anthraquinone core is estimated to be 1.2 nm . Thus, the total length of triphenylene moiety and alkyl chains is expected to be about 3.2 nm . This value is close to the height of the domains obtained from the AFM topography image. Hence we suggest that the anthraquinone moiety is in face-on configuration on the substrate and all the triphenylene moieties are extended away from the substrate in edge-on configuration.

In the AQD6 monolayer, the hydrophilic anthraquinone moiety anchors the molecules at the air-water interface. The limiting area of an edge-on triphenylene unit in the Langmuir monolayer is about 1.1 nm^2 [14, 26]. Hence the area occupied by the assembly of six edge-on triphenylene moieties will be about 6.6 nm^2 . Since this value is close to the limiting area ($A_o = 6.8 \text{ nm}^2$) of the AQD6 molecule (figure 1), we suggest that all the six triphenylene moieties are on an average in the edge-on configuration at air-water interface. Similar conformation of the molecules has been reported for the Langmuir monolayer of molecules with electron rich triphenylene core connected to six triphenylene moieties [13].

The AQD6 monolayer film transferred onto the hydrophilic silicon, had the transfer ratio of about 0.7. Figure 5 shows the AFM topography image of the monolayer film on the silicon substrate.

The line profile on the topography image yielded a height of about 3.4 nm . This suggests that the molecular conformation on the silicon substrate is similar to that on the mica substrate with anthraquinone moiety in face-on configuration and triphenylene moieties in edge-on configuration. Figure 6 shows a schematic diagram of the organization of molecules on silicon substrate.

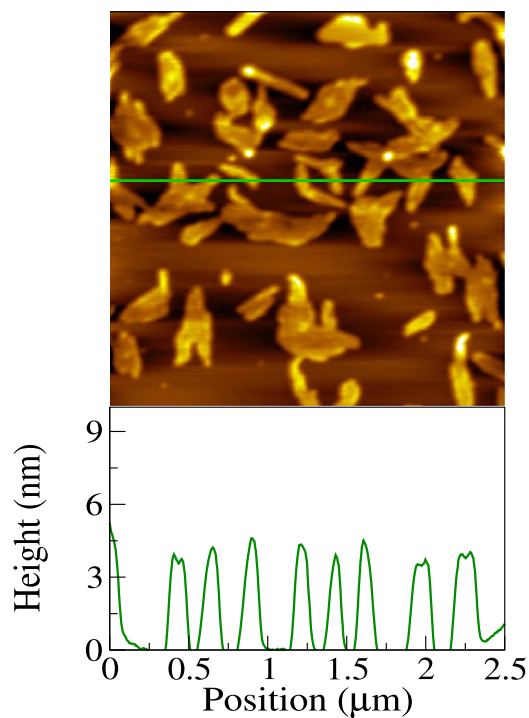


Figure 4. Tapping mode AFM image of AQD6 monolayer on hydrophilic mica sheet. Here the film was transferred at a target pressure of 3.4 mN/m. The line profile yields an average height of 3.5 nm.

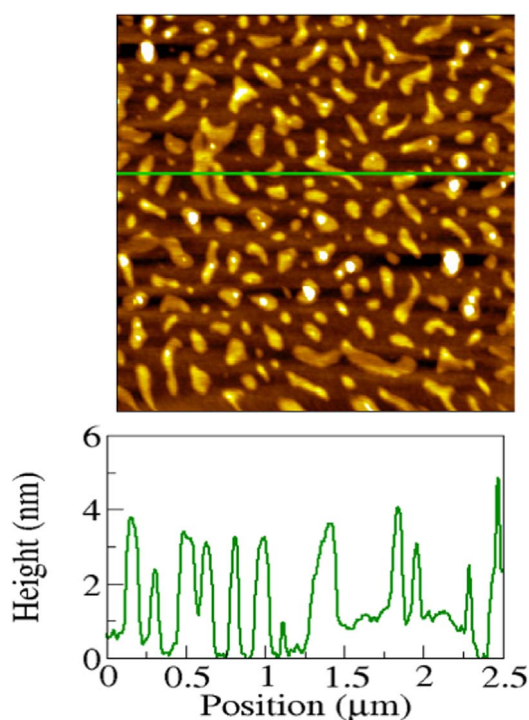
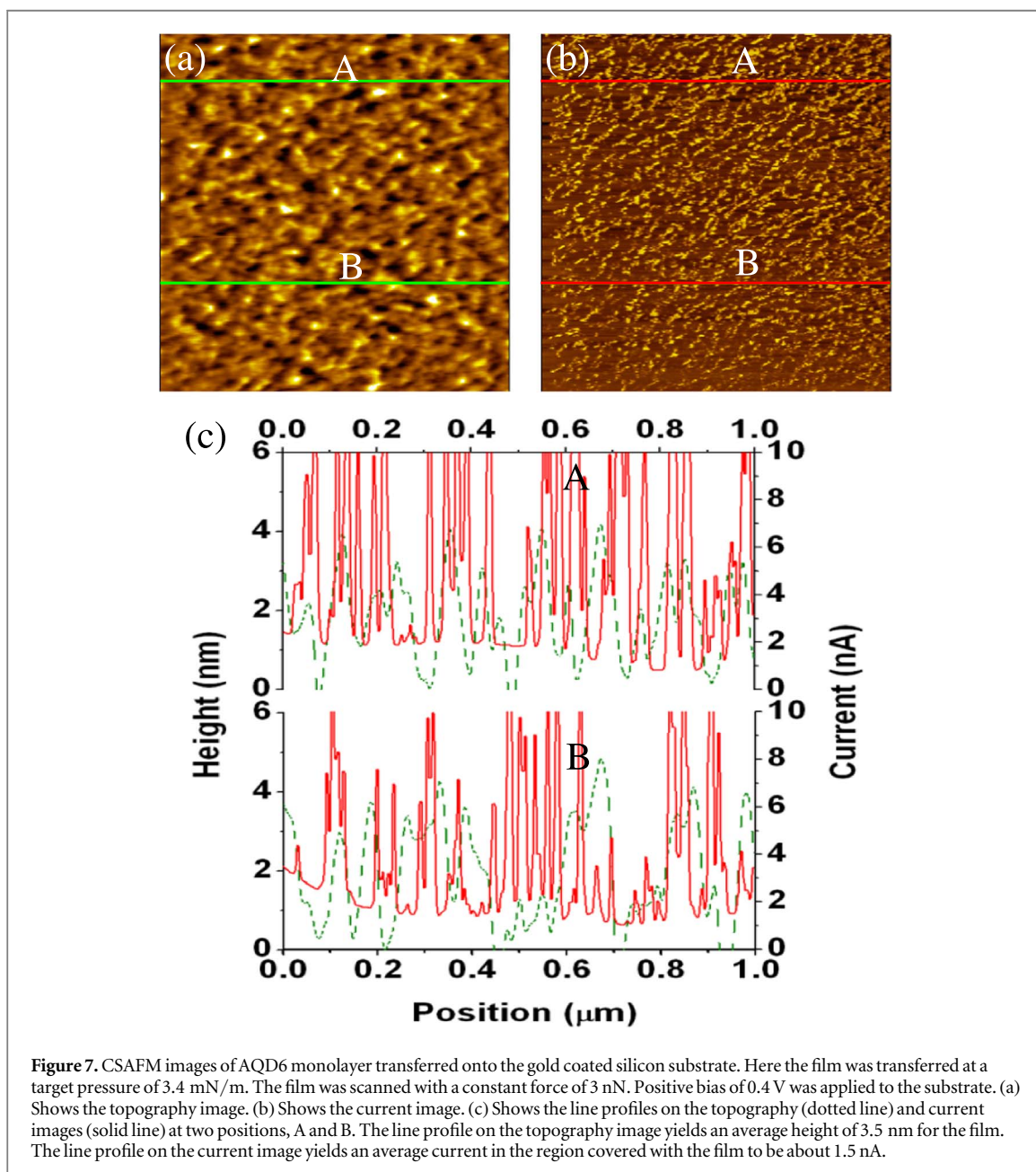
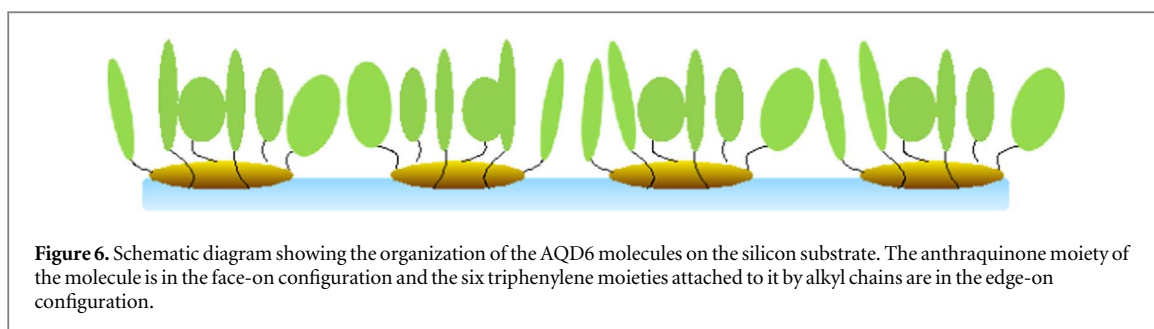


Figure 5. Tapping mode AFM image of AQD6 monolayer on hydrophilic silicon substrate. Here the film was transferred at a target pressure of 3.4 mN/m. The line profile yields an average height of 3.0 nm.

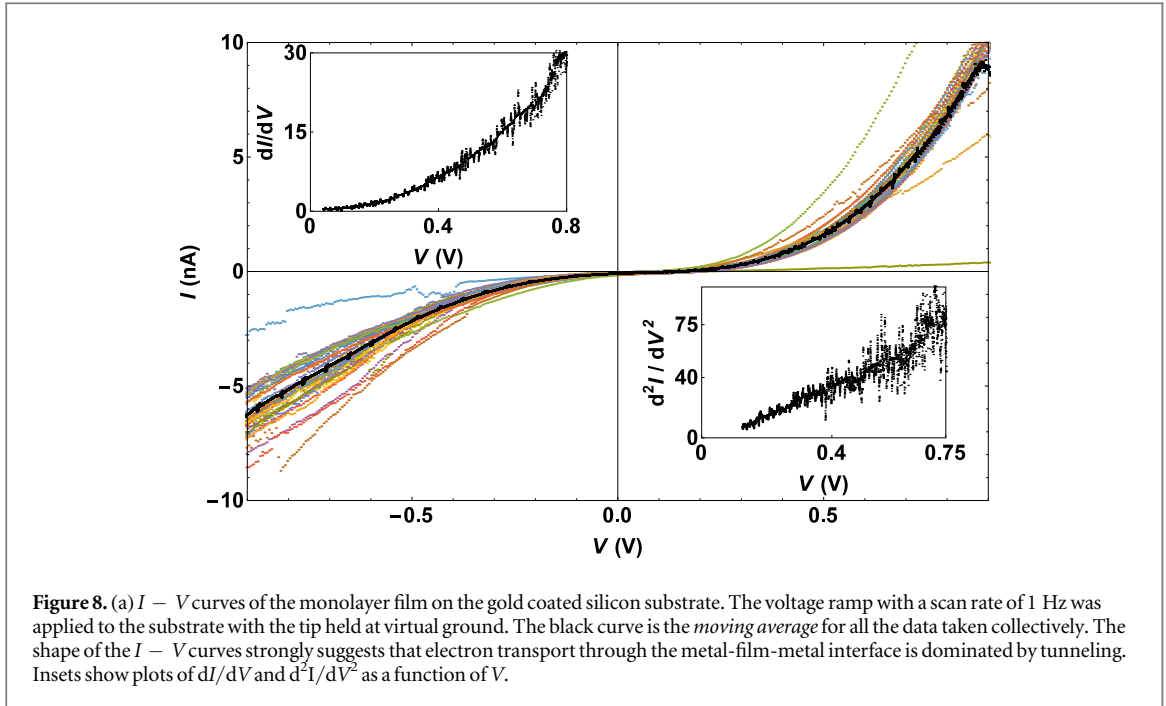
3.3. Electrical conductivity measurements

The ability of the CSAFM to simultaneously get surface topography and electrical conductivity makes it a convenient tool for studying thin film properties [27]. We have employed this technique to study the electrical conductivity of the AQD6 monolayer transferred onto a gold coated silicon substrate. The AQD6 monolayer film between the conducting tip and the metal substrate forms metal-film-metal junction. Positive bias voltage



of 0.4 V was applied to the substrate and the tip was kept at virtual ground. The film was scanned in the contact mode with a constant applied force of 3 nN. Figures 7(a) and 7 show the topography and the corresponding current images, respectively.

The average height of the film measured from the line profile drawn on the topography image was about 3.4 nm. This suggests that the organization of molecules on gold coated silicon substrate is similar to that on the



hydrophilic mica and silicon substrates. The current image 7(b) taken at a bias voltage of 0.4 V yields an average current of about 1.5 nA.

We have carried out the $I - V$ measurements by keeping the conducting tip in contact with the film with a applied force of 3 nN. The tip was kept at the virtual ground and the voltage ramp of -1.0 V to $+1.0$ V was applied to the substrate at a rate of 1 Hz. Figure 8 shows a typical $I - V$ curve. In the vicinity of zero voltage, the current gradually increased and at higher voltages there was a rapid increase in the current. The forward and the reverse bias had a small current offset of about 20–25 pA at zero voltage. This offset is usually attributed to the charging current of the system capacitance [28]. The shape of the $I - V$ curve strongly suggests that there is a potential barrier for the electron transfer between the two electrodes [29]. We find that in our system, dI/dV increases with increase in voltage V (inset in figure 8) suggesting that the charge transfer across the AFM tip-AQD6 film-substrate interface is by tunneling.

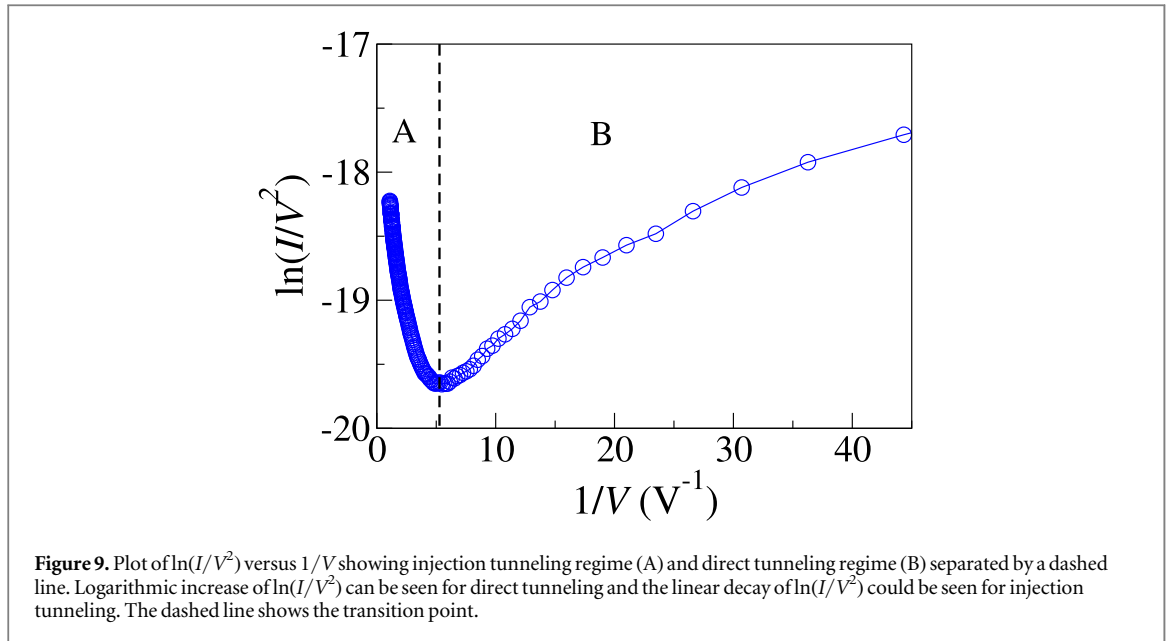
Simmons has derived a generalized formula for the electron tunneling current between two electrodes separated by an insulating film [30]. According to his formula, the $I - V$ relation for the tunneling through the potential barrier of arbitrary shape is given by the equation,

$$I = \frac{eA}{2\pi\hbar d^2} \left[\bar{\phi} \exp\left(-\frac{4\pi\bar{d}\sqrt{2m^*\bar{\phi}}}{\hbar}\right) - (\bar{\phi} + eV) \exp\left(-\frac{4\pi\bar{d}\sqrt{2m^*(\bar{\phi} + eV)}}{\hbar}\right) \right] \quad (2)$$

Here, e is the electron charge, A is the effective electrical contact area between the tip and the film, $\bar{\phi}$ is the mean barrier height, \bar{d} is the mean barrier width, m^* is the effective mass of electron and \hbar is the Planck's constant. For very low applied bias voltage, the potential barrier is approximately of rectangular shape [30]. Here, $\bar{\phi} \approx \phi_0$ and $\bar{d} \approx d$, where ϕ_0 is the height of rectangular barrier and d is the distance between the electrodes. With these approximations [30], equation (2) reduces to,

$$I = \frac{A\sqrt{2m^*\phi_0}}{d} \left(\frac{e}{\hbar}\right)^2 V \exp\left(-\frac{4\pi d\sqrt{2m^*\phi_0}}{\hbar}\right) \quad (3)$$

At intermediate bias voltages ($V < \phi_0/e$), the potential barrier can be considered to be of trapezoidal shape. In this regime, $\bar{\phi} \approx \phi_0 - eV/2$ and $\bar{d} \approx d$. For alkane thiol molecules, it has been shown that the electron transport mechanism at intermediate bias voltages ($V < \phi_0/e$) is by direct tunneling [31]. Direct tunneling refers to the tunneling of the electron from one electrode to the other, without hopping or diffusing into the insulating medium. In the high bias voltage regime ($V > \phi_0/e$), the potential barrier is approximately of triangle shape and is equivalent with the injection tunneling (Fowler-Nordheim tunneling) [19]. Hence it is assumed that $\bar{\phi} \approx \phi_0/2$ and $\bar{d} \approx d\phi_0/(eV)$. The tunneling current for this regime [32] is given by the equation,



$$I = \frac{Ae^3V^2m_e}{8\pi h\phi_o d^2m^*} \exp\left(-\frac{8\pi d\sqrt{2m^*\phi_o^3}}{3heV}\right) \quad (4)$$

Here, m_e is the mass of the free electron. In injection tunneling, the electron is first injected into the insulating medium through the triangular barrier before it is transported to the second electrode. A transition in the electron transport mechanism from the direct tunneling to the injection tunneling is possible, when the value of applied bias voltage is in the vicinity of the barrier height of the film [19]. In direct tunneling, the value of $\ln(I/V^2)$ logarithmically increases with $1/V$ and in injection tunneling, $\ln(I/V^2)$ linearly decreases with $1/V$. Hence a minimum in the variation of $\ln(I/V^2)$ as a function of $1/V$ indicates a transition. The bias voltage corresponding to the transition is called transition voltage (V_{trans}).

A transition in the charge transport mechanism from the direct tunneling to the injection tunneling is possible, when the value of applied bias potential is in the vicinity of the barrier height of the film [19]. In direct tunneling, the value of $\ln(I/V^2)$ increases with $1/V$ and in injection tunneling [31], $\ln(I/V^2)$ linearly decreases with $1/V$ [19]. Hence a minimum in the variation of $\ln(I/V^2)$ as a function of $1/V$ indicates a transition. The bias voltage corresponding to the transition is called transition voltage (V_{trans}).

Figure 9 shows the typical plot of $\ln(I/V^2)$ as a function of $1/V$ for AQD6 monolayer film for the positive bias voltages. We find a transition in the tunneling mechanism, from direct tunneling to injection tunneling, as the bias voltage is varied. In literature, the transition in the electron transport mechanism has been reported in the self-assembled monolayer of π -conjugated thiol molecules [19] and in the purple membrane monolayer [18]. We have indicated the transition from the direct tunneling regime to the injection tunneling regime by a dashed line (figure 9). The corresponding V_{trans} obtained from the relation can be used to estimate the barrier height (ϕ_o) [18]. The average value of ϕ_o obtained from thirty independent $I - V$ measurements taken at different locations over three sample plates was about 0.19 eV with a standard deviation of about 0.02 eV.

The values of the effective mass of electron and effective electrical contact area between the tip and the film can be obtained by analyzing the $I - V$ data in the high voltage regime. In this regime, $\ln(I/V^2)$ varies linearly with $1/V$ and they are related by the following equation (see equation (4)),

$$\ln\left(\frac{I}{V^2}\right) = -\left(\frac{8\pi d\sqrt{2m^*\phi_o^3}}{3he}\right)\left(\frac{1}{V}\right) + \frac{Ae^3m_e}{8\pi h\phi_o d^2m^*} \quad (5)$$

The values of slope and intercept can be obtained by fitting a straight line to the plot of $\ln(I/V^2)$ variation with $(1/V)$ data in the high voltage regime. Substituting the values of slope, ϕ_o , e , h , and d into the expression for slope, the effective mass of electron (m^*) can be calculated. In our system, d corresponds to the thickness of the film (3.4 nm) since the tip is located just at the surface of the film. We obtain the m^* value to be $0.120m_e$ with a standard deviation of about $0.004m_e$. From the intercept of the straight line we have calculated the value of the effective electrical contact area (A) between the tip and the film to be 0.54 nm^2 with a standard deviation of 0.02 nm^2 . The effective mass of the electron calculated is of the same order as obtained for purple membrane corresponding to 2.5 nm [18]. The effective contact area calculated for our metal-film-metal junction is also of the order of values obtained for purple membrane [18].

The V_{trans} calculated for the positive and negative applied bias voltages were different. The value of V_{trans} obtained by applying positive bias voltage to the substrate ($V_{trans}^+ = 0.19 \pm 0.02$ V) was less than the value of V_{trans} obtained when negative bias voltage was applied to the substrate ($V_{trans}^- = 0.34 \pm 0.02$ V). Similar behavior has been reported in the case of π -conjugated thiol system and was attributed to the asymmetry in the two metal-film contacts [19]. The molecules of AQD6 in the LB monolayer were oriented in such a way that the triphenylene moiety was in contact with the conducting tip and the anthraquinone moiety was in contact with the substrate. Hence the electronic states at the gold substrate-film interface arising from the coupling between the electrons of anthraquinone and gold will be different from that of the tip-film interface arising due to the coupling between the electrons of triphenylene and platinum [2]. This asymmetry in the potential barrier between the metal electrodes results in unequal potential drop at the two metal-film interfaces.

We have estimated the ϕ_o value by assuming the potential barrier to be of simple geometrical shape (trapezoidal, triangle) [30]. To get more accurate values of the barrier height, actual potential barrier has to be modeled by considering the structure and organization of the molecules. The HOMO/LUMO levels of the AQD6 molecules are positioned near to the Fermi level of metal electrodes in the metal-film-metal junction. When a small bias potential (<1 V) is applied between the metal electrodes a transition from the direct tunnelling to Fowler-Nordheim tunnelling occurs. Such a transition is not possible in case of alkane thiols because the bias potential necessary for such a transition is high ($\gg 1$ V) which may lead to electrical breakdown of the metal-film-metal junction. In addition there can be differences in the conductivity of the junction depending on whether the film is chemically adsorbed on the metal electrodes or physically adsorbed [38]. In the case of triphenylene discotic core tethered with pyridinium moiety (PyTp) [33], CSAFM studies on the monolayer film has shown that the electron transport is by injection tunneling. Unlike AQD6, PyTp is an ionic molecule. In this system, the packing and supramolecular order drastically influence the electronic properties [8]. The molecular conduction behavior significantly changes not only with the molecular structure but also with the molecular environment [34]. Haiss *et al* [35] have shown the impact of contact morphology and the substrate surface roughness on the molecular conductance. Their experimental studies to determine the electrical conductance of alkanethiol molecules between gold contacts showed three different fundamental conductance values for each molecule. They attributed this to the different adsorption sites of the sulphur on the gold surface. The charge transport in the molecular junctions are also influenced by the polarization of the molecules in the presence of external fields [36]. Such polarization effects in the molecule can provide single molecular switching with the use of only two electrodes. The transition in the tunneling mechanism, from direct tunneling to the injection tunneling, in the metal-monolayer film-metal junction is interesting. Song *et al* [17] have demonstrated that molecular transistors can be created by using molecules which exhibit such transition in the tunneling mechanism. They fabricated devices using 1, 8-octanedithiol and 1, 4-benzenedithiol molecules wherein the molecular orbitals of these molecules can be modulated by an external gate voltage. Insets in the figure 8 show the first and second derivatives of I with respect to V obtained for a typical $I - V$ curve. The non-linear behaviour of the $I - V$ curve is important for device application like electromagnetic radiation detectors. Jeon *et al* [37] have shown that a sensitive THz detector based on metal-semiconductor-metal junction with non-linear $I - V$ characteristics will have sensitivity dependent on the ratio I''/I' , where I'' and I' are the second and first derivatives of I with respect to V , respectively. The rectified voltage output of THz detectors is proportional to the ratio I''/I' . The metal-AQD6 film-metal junction we have studied has a ratio of about 3 which is of the same order as obtained by Jeon *et al* for metal-semiconductor-metal junctions. Our work highlights the possible usage of organic semiconductors/insulators for the devices like THz detectors. Our electrical studies on metal-LB film-metal is important for understanding the mechanism of charge transfer across interfaces and to develop cost effective devices based on metal-organic film interface properties.

4. Conclusions

Monolayer films of a star shaped liquid crystalline molecule made up of anthraquinone and triphenylene moieties were studied at air-water and air-solid interfaces. At air-water interface, the material exhibits stable monolayer which can be transferred onto the solid substrates by LB technique. The limiting area of the molecule in the Langmuir monolayer and the AFM topography image of the monolayer film suggest that the anthraquinone moiety is in face-on configuration on the substrate and the triphenylene moieties are on an average in edge-on configuration extended away from the substrate. The film transferred onto a gold coated silicon substrate was studied using a current sensing atomic force microscope. Our analysis of the $I - V$ characteristics showed a transition in the electron transfer mechanism, from direct tunneling to the injection tunneling, as the applied bias voltage was varied. The bias voltage at which the transition occurs (V_{trans}) was determined from the $\ln(I/V^2)$ versus $1/V$ plot. The V_{trans} value was used to estimate the barrier height (ϕ_o) of the film. For positive bias voltage, the average value of ϕ_o was 0.19 eV with a standard deviation value of 0.02 eV.

From the analysis of the $I - V$ data in the higher voltage regime, we have calculated the effective mass of electron m^* to be $0.12m_e$.

Acknowledgments

B. Kumar acknowledges DST-SERB Early Career Research Award for financial support.

ORCID iDs

Bharat Kumar  <https://orcid.org/0000-0002-7600-5137>

References

- [1] Aviram A and Ratner M A 1974 *Chem. Phys. Lett.* **29** 277–83
- [2] Moth-Poulsen K and Bjørnholm T 2009 *Nat. Nanotechnol.* **4** 551
- [3] Yamamoto Y, Fukushima T, Suna Y, Ishii N, Saeki A, Seki S, Tagawa S, Taniguchi M, Kawai T and Aida T 2006 *Science* **314** 1761–4
- [4] Priyadarshy S, Therien M J and Beratan D N 1996 *J. Am. Chem. Soc.* **118** 1504–10
- [5] Schmidt-Mende L, Fechtenkötter A, Mullen K, Moons E, Friend R H and MacKenzie J D 2001 *Science* **293** 1119–22
- [6] Laursen B W et al 2004 *Langmuir* **20** 4139–46
- [7] Tkachenko N V, Tauber A Y, Hynninen P H, Sharonov A Y and Lemmetyinen H 1999 *J. Phys. Chem. A* **103** 3657–65
- [8] Sergeev S, Pisula W and Geerts Y H 2007 *Chem. Soc. Rev.* **36** 1902–29
- [9] Josefowicz J Y, Maliszewskij N C, Idziak S H J, Heiney P A, McCauley J P and Smith A B 1993 *Science* **260** 323–6
- [10] Schönherr H, Kremer F J B, Kumar S, Rego J A, Wolf H, Ringsdorf H, Jaschke M, Butt H J and Bamberg E 1996 *J. Am. Chem. Soc.* **118** 13051–7
- [11] Charra F and Cousty J 1998 *Phys. Rev. Lett.* **80** 1682
- [12] Tsukruk V V, Bengs H and Ringsdorf H 1996 *Langmuir* **12** 754–7
- [13] Maliszewskij N C, Heiney P A, Josefowicz J Y, Plesniviy T, Ringsdorf H and Schuhmacher P 1995 *Langmuir* **11** 1666–74
- [14] Nayak A, Suresh K A, Pal S K and Kumar S 2007 *J. Phys. Chem. B* **111** 11157–61
- [15] Nayak A and Suresh K 2008 *The Journal of Physical Chemistry B* **112** 2930–6
- [16] Pradeau J P, P H and Armand F 1999 *J. Phys. D: Appl. Phys.* **32** 968
- [17] Song H, Kim Y, Jang Y H, Jeong H, Reed M A and Lee T 2009 *Nature* **462** 1039
- [18] Casuso I, Fumagalli L, Samitier J, Padros E, Reggiani L, Akimov V and Gomila G 2007 *Phys. Rev. E* **76** 041919
- [19] Beebe J M, Kim B, Gadzuk J W, Frisbie C D and Kushmerick J G 2006 *Phys. Rev. Lett.* **97** 026801
- [20] Gayathri H N and Suresh K A 2015 *J. Appl. Phys.* **117** 245311
- [21] Gayathri H N, Kumar B, Suresh K A, Bisoyi H K and Kumar S 2016 *Phys. Chem. Chem. Phys.* **18** 12101
- [22] Kumar S 2009 *Liq. Cryst.* **36** 607–638
- [23] Gupta R K and Suresh K A 2004 *Eur. Phys. J. E* **14** 35
- [24] Davies J T and Rideal E K 1963 *Interfacial Phenomena* (New York: Academic)
- [25] Dervichian D G 1939 *J. Chem. Phys.* **7** 931
- [26] Albrecht O, Cumming W, Kreuder W, Laschewsky A and Ringsdorf H 1986 *Colloid Polym. Sci.* **264** 659–67
- [27] Han D H, Kim J W and Park S M 2006 *J. Phys. Chem. B* **110** 14874
- [28] Mishra P, Karmakar P and Ghose D 2006 *Nucl. Instrum. Methods Phys. Res. B* **243** 16–9
- [29] Xu D, Watt G D, Harb J N and Davis R C 2005 *Nano Lett.* **5** 571–7
- [30] Simmons J G 1963 *J. Appl. Phys.* **34** 1793
- [31] Wang W, Lee T and Reed M A 2003 *Phys. Rev. B* **68** 035416
- [32] Lenzlinger M and Snow E H 1969 *J. Appl. Phys.* **40** 278
- [33] Nayak A and Suresh K A 2008 *Phys. Rev. E* **78** 021606
- [34] Selzer Y, Cai L, Cabassi M A, Yao Y, Tour J M, Mayer T S and Allara D L 2005 *Nano Lett.* **5** 61–5
- [35] Haiss W, Martin S, Leary E, Zalinge H V, Higgins S J, Bouffier L and Nichols R J 2009 *J. Phys. Chem. C* **113** 5823
- [36] Galperin M, Ratner M A, Nitzan A and Troisi A 2008 *Science* **319** 1056
- [37] Jeon Y, Jung S, Jin H, Mo K, Kim K R, Park W K, Han S T and Park K 2017 *Sci. Rep.* **7** 16830
- [38] Akkerman H B and De Boer B 2008 *J. Phys. :Condense.Matter* **20** 013001